Waste Management 100 (2019) 336–345

Contents lists available at ScienceDirect

Waste Management

journal homepage: www.elsevier.com/locate/wasman

Gasification of poultry litter in a lab-scale bubbling fluidised bed reactor: Impact of process parameters on gasifier performance and special focus on tar evolution

Giannis Katsaros [a,*], Daya Shankar Pandey [a,b,*], Alen Horvat [c], Guadalupe Aranda Almansa [e], Lydia E. Fryda [e], James J. Leahy [d], Savvas A. Tassou [a]

[a] RCUK Centre for Sustainable Energy Use in Food Chains (CSEF), Brunel University London, Uxbridge UB8 3PH, UK
[b] School of Engineering and the Built Environment, Anglia Ruskin University, Chelmsford CM1 1SQ, UK
[c] Carlos III University of Madrid, Energy Systems Engineering Group, Thermal and Fluids Engineering Department, Avda. de la Universidad 30, 28911 Leganés, Madrid, Spain
[d] Carbolea Research Group, Department of Chemical Sciences, Bernal Institute, University of Limerick, Limerick V94 T9PX, Ireland
[e] Energy Research Centre of the Netherlands, Biomass and Energy Efficiency, Petten, the Netherlands

ARTICLE INFO

Article history:
Received 5 March 2019
Revised 2 August 2019
Accepted 9 September 2019
Available online 30 September 2019

Keywords:
Poultry litter
Gasification
Bubbling fluidised bed
Tar
Agglomeration

ABSTRACT

Poultry litter (PL) gasification was experimentally investigated using a lab-scale bubbling fluidised bed reactor. Characterisation of the gasification process was performed in terms of yields and compositions of both gas and tar, lower calorific value (LCV) of the product gas, cold gas efficiency (CGE) and carbon conversion efficiency (CCE). Experiments were carried out at different temperatures (700–750 °C) and equivalence ratios (ERs). The effect of gasifier temperature at a constant ER of 0.21 shows that an increase in temperature improved the gasification process performance whilst the total tar content decreased, implying that higher temperature enhances the conversion of biomass to product gas. The total gas yield increased from 0.93 to 1.24 $N_{2\text{-free}}$ $m^3/kg_{feedstock\text{-}daf}$, LCV increased from 3.38 MJ/m^3 to 4.2 MJ/m^3, while the tar content was reduced by 24% (5.6–4.25 $g_{tar}/kg_{feedstock\text{-}daf}$). The detailed analyses of tar compositions reveal that styrene and xylenes were the most abundant compounds in the secondary tar group. Moreover, naphthalene and 1, 2-methyl naphthalene were the dominant compounds found in tertiary polycyclic aromatic hydrocarbons (PAH) and alkyl tertiary groups, respectively. Furthermore, at the highest tested temperature of 750 °C and ER of 0.25, bed agglomeration took place causing the shutdown of the gasifier. The defluidisation of the bed occurred due to the high ash content of PL comprising of low melting temperature alkali compounds. The results obtained from this study showed the performance and potential challenges associated with gasifying PL in a fluidised bed reactor for the combined heat and power production at farm level.

1. Introduction

The production of poultry meat is expanding throughout the world, imposing significant challenges related to the efficient management of associated litter generation. In 2018, on a monthly basis approximately 80 million birds, mostly chickens were slaughtered in the UK alone (Rumsey, 2018). A recent study estimated that the amount of PL produced falls between 1.75 and 5.7 kg of litter/bird over a 42 days production cycle (Dalólio et al., 2017). In the UK, the total amount of PL generated annually ranges between 140,000 and 456,000 tonnes, while its LCV on an as received basis ranges between 8.75 GJ/tonne and 14.27 GJ/tonne (Lynch et al., 2013). Therefore, the estimated potential energy from PL varies between 1.22 PJ and 6.5 PJ. Considering its energy potential, PL can be utilised as a renewable feedstock for bioenergy production.

The growing demand for poultry meat has led to intensive livestock farming which outperformed the prevalent traditional farming based on small installations. Although the intensive farming is

Abbreviations: PL, poultry litter; LCV, lower calorific value; CGE, cold gas efficiency; CCE, carbon conversion efficiency; ER, equivalence ratio; daf, dry ash free; a.r., as received; d.b., dry basis; PAH, polycyclic aromatic hydrocarbons; GC, gas chromatography; ECN, The Energy Centre of the Netherlands; SPA, solid phase adsorption; FID, flame ionisation detector.

* Corresponding authors at: RCUK Centre for Sustainable Energy Use in Food Chains (CSEF), Brunel University London, Uxbridge UB8 3PH, UK (D.S. Pandey).

E-mail addresses: Ioannis.Katsaros@brunel.ac.uk (G. Katsaros), Daya.Pandey@anglia.ac.uk (D.S. Pandey).

https://doi.org/10.1016/j.wasman.2019.09.014
0956-053X/

more efficient and cost effective, it creates serious environmental concerns due to the large amount of waste accumulated within a confined area where the available arable land for manure application as a nutrient source is limited (Bernal et al., 2015). Excessive soil fertilisation with nutrient rich animal manure can lead to eutrophication, nitrate leaching, crop toxicity, odours and emissions of greenhouse gases (NH_3, NO_x, N_2O) to the atmosphere (Billen et al., 2015; Joseph et al., 2012; Lynch et al., 2013; Taupe et al., 2016).

Growing environmental concerns associated with excessive fertilisation demands the development of alternative viable options for treating animal waste. Due to its relatively high energy content and fixed carbon, PL in particular, has gained attention lately in energy conversion processes. Currently two different pathways, biochemical and thermochemical conversion are being exploited. The choice of technology depends on the feedstock properties, the desired end product, economic feasibility and environmental regulations (Pandey et al., 2016). The slow production rate of the anaerobic digestion process, the need for feedstock with high moisture content (moisture content of PL varies significantly from batch to batch and has relatively high solid content) and related high capital costs make this method less suitable for PL treatment (Burra et al., 2016; Joseph et al., 2012). Composting, although producing a fertiliser with a value in the market, poses some serious drawbacks such as the odours generated during the process, the need for land availability and high equipment costs (Joseph et al., 2012). Thermochemical conversion seems a promising option for PL treatment, since it can reduce the volume of the waste by up to 80–95%, upgrade PL to higher value products (e.g. bio-oil, synthetic natural gas), destroy pathogens due to high operating temperatures, while it also offers the possibility of electricity, heat generation and biofuel production (Arena, 2012).

Thermochemical conversion routes are divided into three core technologies, namely combustion, gasification and pyrolysis. Amongst these technologies, combustion is already proven and mature whereas gasification and pyrolysis technologies are still in their early commercialisation stage and pose different challenges that need to be addressed prior to their deployment at full commercial scale. In a gasification process, a carbon-based feedstock is partially oxidised at high temperatures (700–1200 °C) in the presence of an oxidant (air, steam, oxygen, or mixtures thereof) under sub-stoichiometric conditions. The result of this process is the production of a combustible gas known under the different names "producer gas", "product gas" or "syngas" consisting mainly of CO, H_2, CO_2, CH_4 and small amount of C_{2+} compounds, along with impurities, such as fine particulates, tars and alkali metals (Arena, 2012). To maintain consistency, the term "product gas" is used throughout the paper, since "syngas" refers to gas consisting only of H_2 and CO utilised as basis for the production of chemicals and fuels (Arena et al., 2010). The calorific value of the product gas depends on the oxidant supplied, for instance if air is used as an oxidant it results in a low calorific value (4–7 MJ/Nm^3) gas as the product gas is diluted by atmospheric nitrogen (up to 60%) (Arena, 2012).

Gasification of biomass has emerged as a cleaner technology compared to combustion offering higher efficiency and lower gaseous pollutants such as SO_x, NO_x, heavy metals and particulate emissions that are in compliance with emission standards (Arena, 2012; Pan and Pandey, 2016). However, gasifying PL poses significant challenges due to the presence of compounds with low eutectic temperature in its high ash concentration, which that can lead to fluidised bed agglomeration as well as slagging and fouling issues on the heat transfer surfaces and subsequent equipment train (Bartocci et al., 2017).

Different type of reactors can be employed in a gasification process, namely fixed bed, fluidised bed and entrained flow. Among the various reactors considered, fluidised bed reactors have gained attention recently as they offer greater fuel flexibility and are able to maintain the temperature below the ash melting point, secure high heat transfer rates, achieve a higher production capacity and are suitable in wider range of applications (Belgiorno et al., 2003).

High interest in PL valorisation as a gasification feedstock together with the specific challenges of this fuel is reflected in the large number of publications in the recent years. The effect of limestone addition to prevent agglomeration while gasifying PL has been studied. The authors reported that by adding limestone, agglomeration did not occur below 800 °C compared to the case without limestone where agglomeration was observed at 750 °C (Pandey et al., 2016). The effect of ash composition on PL gasification has been investigated in a pre-pilot reactor by comparing two batches of manure taken from an industrial chicken farm. The experiments were carried out at different ERs (0.27–0.4) and temperatures (700–800 °C). The findings revealed the role of ash composition, since all the process parameters were significantly reduced in the batch with the higher ash content (Di Gregorio et al., 2014). A recent study focused on producing energy from an innovative 300 kW thermal power gasification plant installed on a poultry farm located in central Italy. Aspen Plus v.8.0 model was developed by the authors to predict the outlet gas composition and its LCV which was found in the range 3–5 MJ/m^3 for an ER of 0.2 (Cavalaglio et al., 2018). Six different model based energy integration schemes were applied to a small-scale gasification process for onsite power generation. The findings revealed CGE and exergetic efficiency ranging between 58.4–79.5% and 46.8–65.7% respectively (Font Palma and Martin, 2013). The techno-economic feasibility of generating biochar, electricity and heat production from PL was investigated using a model developed on ECLIPSE software. The authors concluded that gate fees, carbon credits and renewable energy certificates greatly influence the breakeven selling price of produced biochar (Huang et al., 2015).

One of the largest technical obstacles that hinders further development and commercialisation of gasification technology is the presence of tar in the product gas. Tar is a mixture of complex hydrocarbons which may condense in the process installation if the temperature drops below the tar dew point. Condensation of tar leads to the formation of a black and sticky material which causes system malfunctioning due to clogging and fouling. Multiple definitions of tar can be found across literature. One of the most representative definition given by Basu (2010) is the one derived from IEA's gasification task force which defines tar as "the organics produced under thermal or partial-oxidation regimes (gasification) of any organic material, are called tar and are generally assumed to be largely aromatic".

There are two different tar classifications considered, either based on the temperature regime under which tar compounds are formed (Milne et al., 1997) or based on water solubility, dew point temperature, and aromatic ring number (Kiel et al., 2004). According to Milne et al. (1997), tar is classified in primary, secondary, alkyl tertiary and tertiary tar groups. Primary tar derives from pyrolysis reactions of lingo-cellulosic materials at temperatures between 200 and 500 °C. Primary tar consists of highly oxygenated compounds such as acids, sugars, alcohols, and ketones (Horvat et al., 2016c). As the temperature increases and with the presence of the gasification agent, primary tar releases functional groups and reforms into light non-condensable gases and heavier compounds called secondary tar such as phenols and olefins which remain stable up to the temperature of 750 °C. Above 750 °C the secondary tar undergo rearrangement into tertiary tar by completing the condensation pathway resulting in purely aromatic species (Rios et al., 2018). Tertiary tar consists mainly of polycyclic aromatic compounds (PAHs) such as naphthalene, acenaphthylene, and pyrene. PAHs increase exponentially with temperature due

to polymerisation. Alkyl tertiary tar such as methyl naphthalene and biphenyl are intermediates between secondary and PAH tar. The yield of PAHs appears to peak at 850 °C followed by a gradual decrease (Rios et al., 2018; Van Paasen and Kiel, 2004). Tertiary tar is not present in the initial biomass but rather as a product of decomposition and rearrangement of secondary tar. Typically tertiary and primary tar do not co-exist in the reactor (Molino et al., 2016; Rios et al., 2018) nevertheless, in some reactor arrangements this scenario is possible.

Fluidised bed gasifiers generate a blend of secondary and tertiary tar groups in the order of 10 g/Nm^3 (Rabou et al., 2009). Furthermore depending on the end-use application, different tar concentration limits are in place. As an example if the product gas is supplied in internal combustion engines tar limits are in the range of 50–100 mg/Nm^3. Different product gas applications and the respective limits in tar are given in Rios et al. (2018). When the amount of tar is excessive gas cleaning is imperative, which increases the process complexity and costs. In addition to the total amount of tar, the nature of the individual tar compounds is a crucial parameter. The nature of these compounds determines the tar dew point, a decisive factor for downstream applications. In general, the presence of tar compounds with higher molecular weight tends to increase tar dew point and vice versa.

In the recent past PL gasification has been studied extensively but most of the studies have focused on the composition and calorific value of the product gas. The present work apart from studying the effect of temperature on various process parameters (LCV, CGE, CCE etc.), also aims to give a useful insight into the amount and composition of tar derived from PL gasification in a fluidised bed reactor. To the best of authors' knowledge, detailed analysis of the tar generated from PL does not exist in the literature. The temperature range used in this work was chosen based on the findings of previous researchers taking into the consideration of the challenges associated with de-fluidisation and agglomeration of the bed during the PL gasification (Pandey et al., 2016; Taupe et al., 2016; Di Gregorio et al., 2014). Overall, the findings of this study reveal an effective method of managing the unavoidable waste generated and additionally they can be helpful in examining a potential application of the product gas for heat and power generation at a farm level.

2. Experimental

2.1. Materials

PL is a blend of poultry excreta, waste feed, feathers and bedding material such as straw, peat or sand. PL was collected from a local poultry farm in Finland and it was partially dried and sieved to a particle size range of 0.5–0.98 mm before being fed into the reactor. Table 1 reports the ultimate and proximate analysis along with the chemical composition of PL ash. Fixed carbon was calculated by subtracting the percentages of volatile matter and ash from 100% on a dry basis (d.b.). Similarly, the oxygen content was determined by the difference from the elements presented in ultimate analysis. For the determination of the chemical composition of PL ash (generated at 550 °C according to BS EN 14775:2009), the generated ash was digested and analysed using an Agilent Inductively Coupled Plasma-optical emission spectrometry. The ash contained high concentrations of alkali metals such as K and Na that promote agglomeration and consequently can cause disruption of continuous fluidised bed gasification. These alkali metals along with the high concentration of Cl in PL contribute significantly to the potential challenges associated with fouling, agglomeration and corrosion.

2.2. Experimental facility

The experimental set up illustrated in Fig. 1 is located at the Energy Research Centre of the Netherlands (ECN part of TNO). The experimental campaign was carried out under the framework

Table 1
Ultimate, proximate analyses of PL and chemical composition of PL ash.

Proximate analysis (wt. %)			
Moisture (a.r.)		9.70	
Ash content (d.b.)		14.30	
Volatile matter (d.b.)		69.60	
Fixed carbon* (d.b.)		16.10	
Ultimate analysis (wt.%, d.b.)			
Carbon		42.8	
Hydrogen		5.5	
Nitrogen		3.9	
Sulphur		0.60	
Chlorine		0.25	
Oxygen*		32.65	
LHV (in MJ/kg)		16.78	
Chemical composition of PL ash			
Major elements		Minor elements	
Elements	Amount (mg/kg, d.b.)	Elements	Amount (mg/kg, d.b.)
Aluminium (Al)	1200	Arsenic (As)	<0.50
Calcium (Ca)	15,500	Barium (Ba)	29.0
Iron (Fe)	1600	Cadmium (Cd)	0.14
Magnesium (Mg)	8200	Cobalt (Co)	1.90
Manganese (Mn)	600	Chromium (Cr)	16.0
Phosphorous (P)	10,200	Copper (Cu)	84.0
Potassium (K)	27,700	Mercury (Hg)	<0.02
Silicon (Si)	7300	Molybdenum (Mo)	4.80
Sodium (Na)	4200	Nickel (Ni)	16.0
Sulphur (S)	6100	Lead (Pb)	1.50
Titanium (Ti)	95	Antimony (Sb)	<0.50
Zinc (Zn)	450	Thallium (Tl)	<0.50
		Vanadium (V)	4.20

*Calculated by difference; Oxygen = 100-(C + H + N + S + Cl + Ash content); Fixed carbon = 100 − (Volatile matter + Ash content).

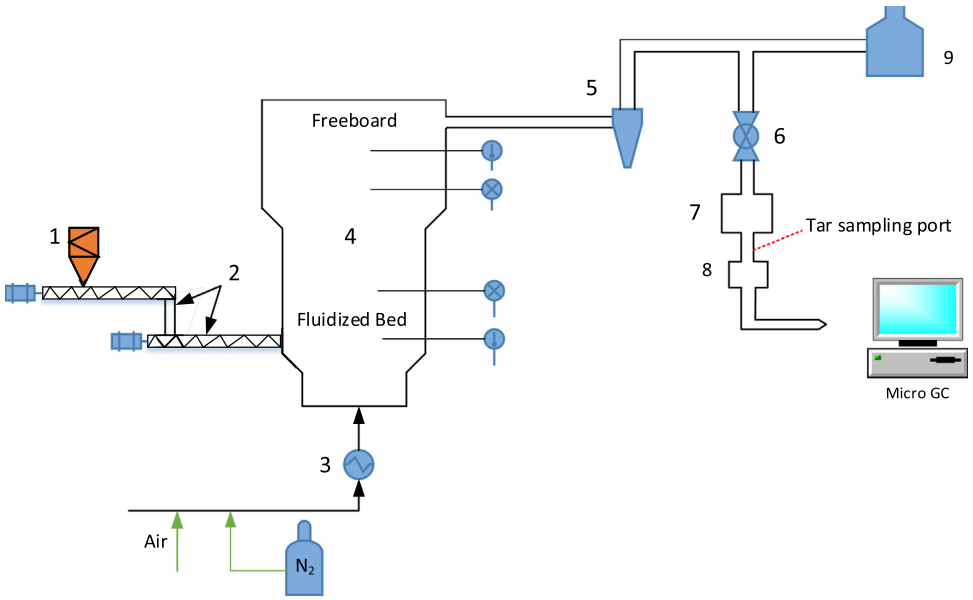

Fig. 1. Lab-scale experimental facility at ECN part of TNO, Netherlands 1: Hopper, 2: Screw feeders, 3: Pre-heater, 4: Gasifier, 5: Cyclone, 6: Valve, 7: Hot filter, 8: Cold filter, 9: Flare.

of the European project BRISK2. Fuel is fed into an atmospheric bubbling fluidised bed reactor by two mechanical screw feeders under 1 Nl/min flow of N_2 (flush gas) in order to avoid backflow of gases. The reactor consists of two different zones: (i) bed section with an internal diameter of 74 mm and 500 mm height and (ii) the freeboard section with an internal diameter of 108 mm and height of 600 mm. The lab-scale reactor operates in allothermal mode, implying that the desired temperature cannot be achieved by controlling the ER alone. Therefore external heat source is needed, which was realised by electrical means under inert conditions. The fluidising medium (a mixture of N_2 and air calculated to achieve a particular ER value while maintaining a constant fluidisation velocity) is adjusted and introduced from the bottom of the reactor through the perforated distributor plate. The fluidising medium is preheated to 160 °C before being introduced into the reactor. The product gas exits the freeboard section passing through a cyclone where entrained particles of char and ash were removed. After the cyclone, part of the raw product gas is sampled for chemical analysis, while the rest is combusted in a flare. Product gas for chemical analysis flows through the hot filter to remove the finest particles that escape from the cyclone. The downstream section of the reactor including a hot filter is maintained at 400 °C, preventing tar condensation inside the pipes. Tar and moisture samples were collected via a sampling port located after the hot filter. Successive cold filter removes tar prior to an online micro-gas chromatography (GC) analyser.

2.3. Test procedure

Considering the high ash content in PL and possible agglomeration issues, experiments were conducted at lower temperature starting from 700 °C. Air and N_2 were continuously supplied from the bottom of the reactor at a total flow rate of 12 Nl/min in order to maintain an adequate fluidisation regime while ensuring the set gasification conditions. The minimum theoretical fluidisation velocity at the specified operating conditions was calculated using correlation proposed by Wen and Yu (1966). Experiments were conducted at different ERs (adjusting the flow rates of air and N_2) and temperatures whilst keeping the same fluidisation condition (fluidisation velocity 4.2 times the minimum one). To adjust for lower ER, the flow rate of air was reduced while the N_2 flow was increased and vice versa. Sieved silica sand (0.25–0.5 mm) was used as the bed material with bulk and absolute densities of 1422 kg/m^3 and 2620 kg/m^3, respectively. To avoid accumulation of ash in the bed (which would distort the results, due to the potential catalytic activity of certain compounds in the fuel ash), 1.06 kg of fresh silica sand was introduced into the reactor on each experimental day.

In order to ensure stable, representative conditions for the calculation of the performance parameters, each test lasted at least 1.5 h. Three different ER levels were tested at each temperature (tests 1–3 at 700 °C and tests 5–7 at 750 °C). Due to time limitations, only one ER was tested at 725 °C (test 4). No sign of agglomeration was observed at this point. The tests at 750 °C and ERs of 0.17 and 0.21 were successfully completed (5, 6) however, during the final test at an ER of 0.25 (test 7), fluctuations of bed temperature and pressure indicated bed agglomeration. A summary of the experimental tests are illustrated in Table 2.

2.4. Measurement methods

Continuous online measurement of product gas composition was carried out by an ABB gas analyser (CO, CO_2, CH_4, H_2, O_2) and Varian micro-GC analysis (Ar/O_2, Ne, N_2, CO, CO_2, CH_4, C_2H_2, C_2H_4, C_2H_6, C_6H_6, C_7H_8, H_2S, and COS). The micro-GC measurements took place continuously at 4 min intervals. Neon (10 ml/min) was added as a tracer gas to measure the flow rate of dry product gas enabling the calculation of carbon conversion, gas yield and cold gas efficiency. The product gas flow rate was calculated according to the formula proposed by Pandey et al. (2016).

The solid phase adsorption (SPA) method was employed for the tar sampling. The SPA protocol coupled with GC detection offers reliable measurement of phenolic and 2–5 rings PAH tar compounds (Horvat et al., 2016b; Rabou et al., 2009). However, SPA is not ideally suitable for the detection of hydrocarbons too heavy to pass through GC instrument. Notable deviations were also observed during the measurement of light hydrocarbons such as benzene and toluene. This may be attributed to their high volatility making these compounds difficult to trap on the solid sorbent (Padban et al., 2000). Three SPA samples were taken for each test

Table 2
Process conditions of the experimental tests.

Type of feedstock	PL						
Test number	1	2	3	4	5	6	7
Feedstock flow rate (kg/h, a.r)		0.548			0.548		
Equivalence ratio, ER (-)	0.17	0.21	0.25	0.21	0.17	0.21	0.25
Air flow rate (Nl/min)	6.05	7.6	9.08	7.6	6.05	7.6	9.08
Nitrogen flow rate (Nl/min)	5.95	4.4	2.92	4.4	5.95	4.4	2.92
Minimum fluidisation velocity U_{mf} (m/s)	0.033	0.033	0.033	0.033	0.033	0.033	0.033
Superficial fluidisation velocity U (m/s)	0.138	0.138	0.138	0.138	0.138	0.138	0.138
Gasifier temperature (°C)	700	700	700	725	750	750	750

condition. 100 ml of dry product gas was withdrawn from the SPA sampling port with an automatic syringe pump. The amount of total GC-detectable tar as well as the amount of each individual tar compound is expressed as an average of the three repetitive measurements. The SPA tar samples were taken in 2 min intervals where the tar vapours either adsorbed or condensed on 500 mg of amino propyl silica sorbent. These tars were subsequently desorbed from the amino phase by the addition of 3×600 ml of dichloromethane before being analysed by gas chromatography.

An Agilent 7890A GC coupled with a triple-axis MSD 5975C was used for identification of the most abundant tar compounds. A Thermo Scientific Trace 1310 GC with a flame ionisation detector (GC-FID) was used for tar quantification. Tert-butylcyclohexane was added to the tar solutions as internal standard. The GC-FID instrument was calibrated by known concentrations of naphthalene/*tert*-butylcyclohexane for quantification of tar chromatograms. A more detailed description of the sampling and extraction processes along with the equipment used can be found elsewhere (Horvat et al., 2016a). Total GC-detectable tar reported in this study refers to the sum of tar compounds eluting from thiophene (M ~84 g/mol) to benzo[*a*]anthracene (M ~ 228 g/mol). Benzene and toluene yields were measured by micro-GC and presented as permanent gases and not as tar compounds (Devi et al., 2005b). The tar yields are reported on a mass basis (g_{tar}/kg $_{feedstock\text{-}daf}$) in order to avoid any dilution effect due to changes in ER. Alternatively, tar yields can be reported on a volumetric basis as $g_{tar}/Nm^3_{dry\ gas}$. The volumetric basis is suitable for industrial developers where upper tar limits with regard to downstream applications need to be met.

2.5. Performance analysis

The process performance parameters analysed in this section as a function of temperature are described below. It should be noted that all calculations were performed on a dry basis and that the concentration of permanent gases includes benzene and toluene but excludes tar compounds. The performance parameters are LCV of product gas, CGE, CCE, gas yield and tar yield. The gasification performance is usually determined by CGE and CCE. CGE is defined as the ratio between the chemical energy of the product gas and the chemical energy of the fuel input. CCE reads as the amount of carbon in the reactor which was converted into the gaseous products.

3. Results and discussion

A summary of the main results for the gasification conditions investigated is given in Table S1 (supplementary file). The results include permanent gas composition, total amount of tar, moisture content in the gas, along with calculated process performance parameters CGE and CCE. The quantities of permanent gas compounds are expressed as an average of four consecutive measurements. It is important to mention that the total gas volume includes both the N_2 contained in air, together with the varying external addition of N_2 which is applied to ensure proper fluidisation. Although, some measurements were taken at 750 °C and an ER = 0.25, the experimental results are not included in Table S1 since agglomeration occurred immediately after steady state conditions were achieved. The detailed information on agglomeration is provided in Section 3.4.

3.1. Composition of the product gas

Fig. 2(a) presents the composition of the major gas components as a function of temperature at a constant ER (0.21). The concentrations of H_2, CO and CH_4 increase with temperature, while the CO_2 content shows the opposite trend. These tendencies stem from the fact that higher temperatures favour char gasification reactions ($C + H_2O <=> CO + H_2$, $C + CO_2 <=> 2\ CO$). CH_4 is mainly evolved during the devolatilisation process. Therefore an increase in CH_4 concentration at higher temperatures might indicate a larger extent of devolatilisation and tar decomposition into lighter molecules such as CH_4. Taupe et al. (2016) reported that at higher temperatures the hydrogen content rises because oxygen reacts preferably with carbon forming CO_2 rather than water. On the other hand the decrease in CO_2 concentration can be attributed to the Boudouard equilibrium ($C + CO_2 <=> 2CO$). The results obtained are in line with the relevant literature (Nilsson et al., 2016; Pandey et al., 2016; Taupe et al., 2016). The evolution of minor gas components is presented in Fig. 2(b). C_2H_4 shows an increasing trend with rising temperature. The decline in ethane (C_2H_6) concentration may be the result of thermal reforming into C_2H_4 and C_2H_2 at elevated temperatures (Pandey et al., 2016; Taupe et al., 2016). C_6H_6 increases slightly with temperature, whilst the concentration of C_7H_8 shows the opposite trend. The increase in C_6H_6 concentration may be attributed to the conversion of phenols and toluene via demethylation (Dufour et al., 2011; Horvat et al., 2016c). C_6H_6 is a thermally stable compound. For its decomposition, an adequate gas residence time and temperatures above 1100 °C are required (Van Paasen and Kiel, 2004). The results of minor gas compounds are in agreement with Xue et al. (2014) where the authors investigated the gasification of raw and torrefied *miscanthus* × *giganteus* at temperatures between 660 and 850 °C and an ER of 0.18–0.32. Sulphur is present in the gas phase mainly in the form of H_2S and COS. There are likely traces of other S compounds, such as thiophenes and mercaptans present in the gas, but those were not measured during the tests. The H_2S increases with temperature while the concentration of the COS is very small and showed almost a negligible change with temperature, hence it is not reported in the graph.

3.2. Gas yield, CCE, CGE, and LCV

Fig. 3(a) shows gas yield and CCE as a function of temperature at a constant ER (0.21). Gas yield is reported on a N_2 and dry ash free basis in order to ascertain the actual gas production without any

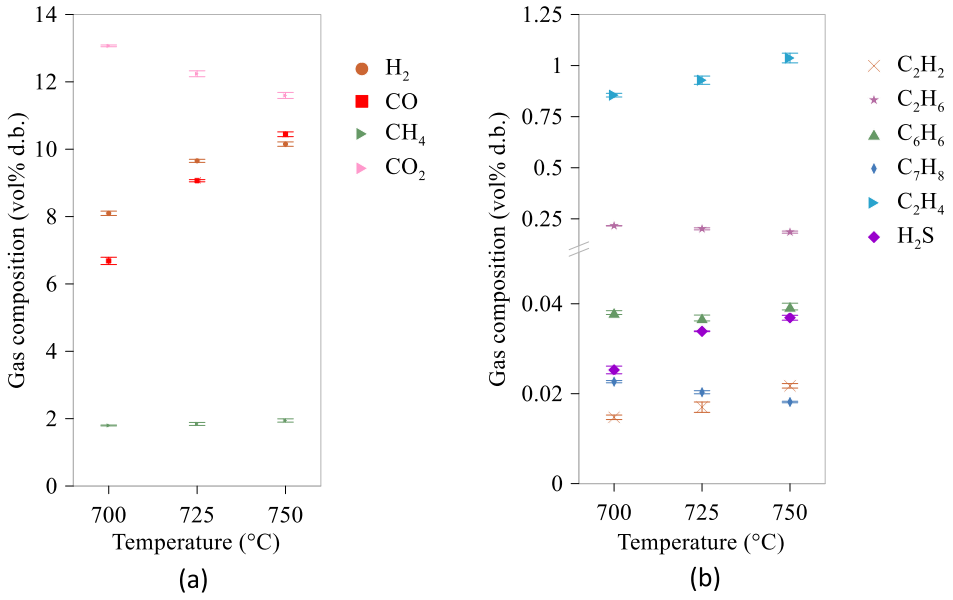

Fig. 2. Effect of temperature on the evolution of (a) dominant gas compounds and (b) minor gas compounds (constant ER = 0.21).

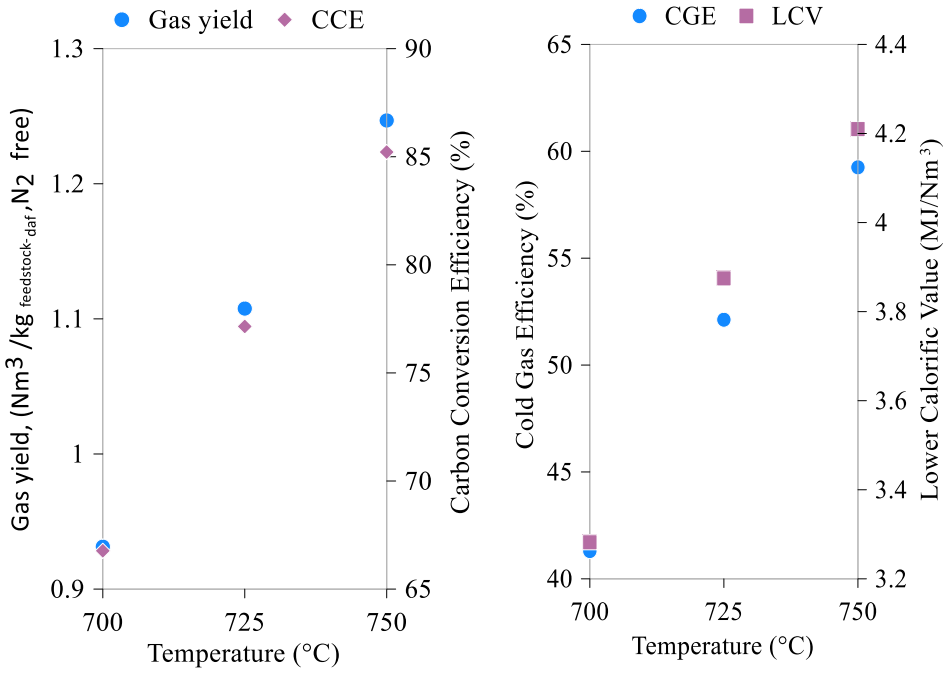

Fig. 3. Effect of temperature at ER = 0.21 on a) gas yield and CCE (b) CGE and LCV.

dilution effects. A gas yield increment of 33% (from 0.93 to 1.24 N_2 free $m^3/kg_{\ feedstock\text{-}daf}$) correlates with elevated temperature. Higher temperature favours the breakdown of molecular bonds (i.e. char conversion and release of volatiles). CCE also rises with temperature from 67% to 85% (an increase of 27%). It should be mentioned that for the experiment conducted at 750 °C and an ER of 0.21, some extraction of bed material took place prior to the test due to ash accumulation in the bed, which may underestimate the carbon conversion. In industrial gasifiers bed extraction usually takes place in order to prevent agglomeration phenomenon due to the build-up of alkaline metals contained in the ash (Nilsson et al., 2016).

Fig. 3(b) depicts the effect of temperature on LCV and CGE at a constant ER (0.21). The LCV of the product gas rises by 24% ranging from 3.4 MJ/Nm^3 to 4.2 MJ/Nm^3 as the temperature increases. It is noteworthy to mention that the highest LCV at 750 °C (4.2 MJ/m^3) doesn't exceed the limit of 4.71 MJ/m^3 reported to be suitable for internal combustion engine applications (Kim et al., 2013). However, the sum of all tar content represented solely as naphthalene gives a LCV of 5.85 MJ/Nm^3. Similarly, Arena and Di Gregorio (2014) in their study on gasification of industrial plastic wastes reported a significant increase in the LCV of the product gas when adding up the energy stored in the tar (i.e. naphthalene). Therefore it is evident that, when tar is removed from product gas, its calorific value reduces significantly. CGE rises considerably with temperature, reaching the value of approximately 60% at the highest tested temperature. The explanation stems from the fact that both gas yield and LCV increase with temperature as described above.

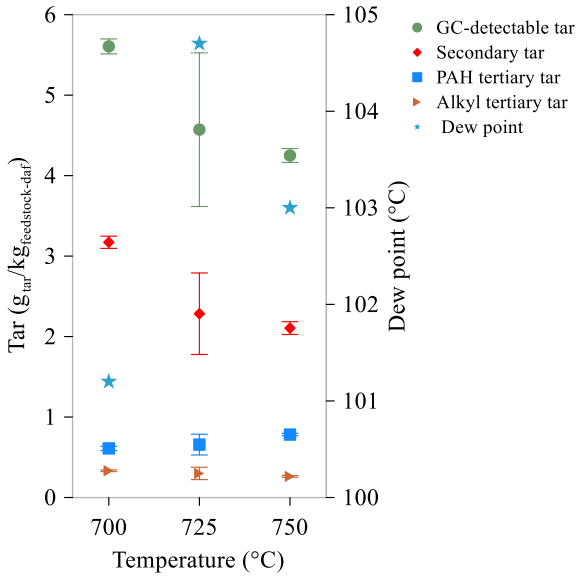

Fig. 4. Effect of temperature on total GC-detectable tar, secondary, alkyl tertiary and PAH tertiary tar group at an ER of 0.21.

3.3. Tar content and composition

The identified tar compounds in this work together with their retention times are given in Table S2 (supplementary file). Compound classification is based on the system proposed by Milne et al. (1997). Compared to typical lignocellulosic biomass, PL is expected to give lower tar yields due to the lower lignin content in PL with respect to wood. Lignin is considered as a tar precursor leading to the formation of higher amount of GC-detectable tar and PAHs (Horvat et al., 2016c; Yu et al., 2014). Furthermore, high alkali and alkali earth metal content (e.g. calcium, magnesium, sodium) in PL ash should catalyse tar cracking reactions. The tar composition of PL feedstock also varies with respect to lignocellulosic feedstock. In particular the high nitrogen content found in waste feed, excreta, and feathers, leads to the formation of nitrogen-containing hydrocarbons (pyridine, pyrrole, methyl pyridine).

The evolution of total GC-detectable tar and associated tar groups as a function of temperature is presented in Fig. 4 (see Tables S3–S5 in supplementary file). Total GC-detectable tar accounts for ~1 wt% of the initial dry and ash free feedstock. For the temperature range tested, the total GC-detectable tar decreased by 24% (from 5.6 to 4.25 $g_{tar}/kg_{feedstock-daf}$). Detected but not identified tar compounds account for 20–30% of total GC-detectable tar. The yield of secondary tar dominates the tar groups while alkyl tertiary tar is the least abundant category over the entire range of tested temperatures. The alkyl tertiary tar group evolves at 750–850 °C as an intermediate between secondary and PAH tertiary tar. At temperatures between 850 and 950 °C, alkyl tertiary tar reforms into unsubstituted PAHs (Van Paasen and Kiel, 2004). Since the temperature range investigated was limited to the range 700–750 °C in order to avoid agglomeration issues it is not possible to verify the evolution profiles of alkyl/PAH tertiary tar in details. However, the yield of PAH tertiary tar group increased by 28% as the temperature increased from 700 to 750 °C and PAH tertiary tar is expected to increase exponentially at higher temperatures. Two different reaction pathways are proposed for the production of PAH tertiary tar. The first pathway describes cracking of heavier hydrocarbons which were not GC-detectable due to their high molecular weight. The second pathway suggests PAH production via decomposition and subsequent recombination of secondary tar or through isomerisation of unsaturated C_2-C_4 hydrocarbons.

The dew points were calculated using an online tool developed by the ECN ("Tar dew point") to be between 101 and 105 °C and show minor effects of tested temperatures on its values. However, the high tar dew points confirm the need for gas cleaning if the gas is to be used in e.g. internal combustion engines, gas turbines or synthesis processes. The dominant factor determining tar dew point is the yield of the PAH compounds in the product gas. The dew point of PAHs correlates with their molecular mass and concentrations in the product gas. Thus, PAH growth amplifies the risk of tar condensation on the cold surfaces of the gasifier.

Fig. 5 shows the evolution of the most abundant individual tar compounds. Secondary tar compounds are represented by oxygen-containing phenolic compounds and substituted one-ring aromatics presented in Fig. 5(a), and nitrogen-containing hydrocarbons displayed in Fig. 5(b). Compounds representing alkyl and PAH tertiary tar groups are shown in Fig. 5(c) and (d), respectively. Note that isomeric compounds such as 1-methyl naphthalene and 2-methyl naphthalene are summed up and presented as a single quantity. Tar data points at 725 °C appear to deviate more than tar data measured at 700 and 750 °C. Such deviation has been reported previously while using SPA method by (Israelsson et al., 2013) and (Neubert et al., 2017). This could result from inconsistencies in feedstock feeding rate, SPA sampling failures such as leaks and clogs or inconsistent integration of complex tar chromatograms.

Horvat et al. (2016c) gasified raw and torrefied *Miscanthus* × *giganteus* at temperatures between 660 and 850 °C. They reported a peak in phenolic yield at 750 °C when using torrefied feedstock. While testing raw feedstock, phenolic yield decreased steeply at temperature above 715 °C. Dufour et al. (2011) conducted pyrolysis experiments on wood chips at temperatures 700–1000 °C and a gas residence time of 2 s. Their findings revealed a decrease in phenol and cresol concentrations as the temperature increased. The authors suggested that phenol is converted into benzene, indene and naphthalene via cyclopentadienyl radicals, while cresol transforms into phenol and toluene through demethylation and dehydration reactions. Willow and beech wood were gasified in a lab-scale fluidised bed reactor. Authors suggested that the conversion of phenol and cresol occurs between 750 and 850 °C (Van Paasen and Kiel, 2004). However, in the present study phenolic hydrocarbons start to decrease earlier at 700 °C. Single-ring aromatics such as styrene and xylenes show a small reduction with temperature, while indene increases slightly. Indene is formed by the decomposition of phenol via cyclopentadienyl radicals. It is probably reformed to either benzene or naphthalene at temperatures higher than the ones tested in the present work, namely between 800 and 900 °C according to Dufour et al. (2011) and (Van Paasen and Kiel, 2004).

Nitrogen-containing hydrocarbons show different thermal behaviour. Pyridine increases steadily while the concentration of pyrrole reduces significantly. Methyl pyridine shows a very small decrease, ranging approximately to 0.12 $g/kg_{feedstock-daf}$. The opposite trends for pyridine and pyrrole may be attributed to the higher thermal stability of the former compound. Zhao et al. (2010) investigated the transformation of nitrogen during pyrolysis and combustion of coal in a flow reactor. Pyridine and pyrrole were considered as model compounds while measuring the amount of H_2 and HCN in order to identify their thermal stability. The findings revealed that that pyridine appeared to be more stable generating high amounts of HCN at 825 °C, while the respective temperature for pyrrole was at 775 °C.

Methyl naphthalene is the most abundant of the alkyl tertiary tar compounds, indicating decreased yields in the tested temperature range. Biphenyl yield remains constant, while 2-ethenyl naph-

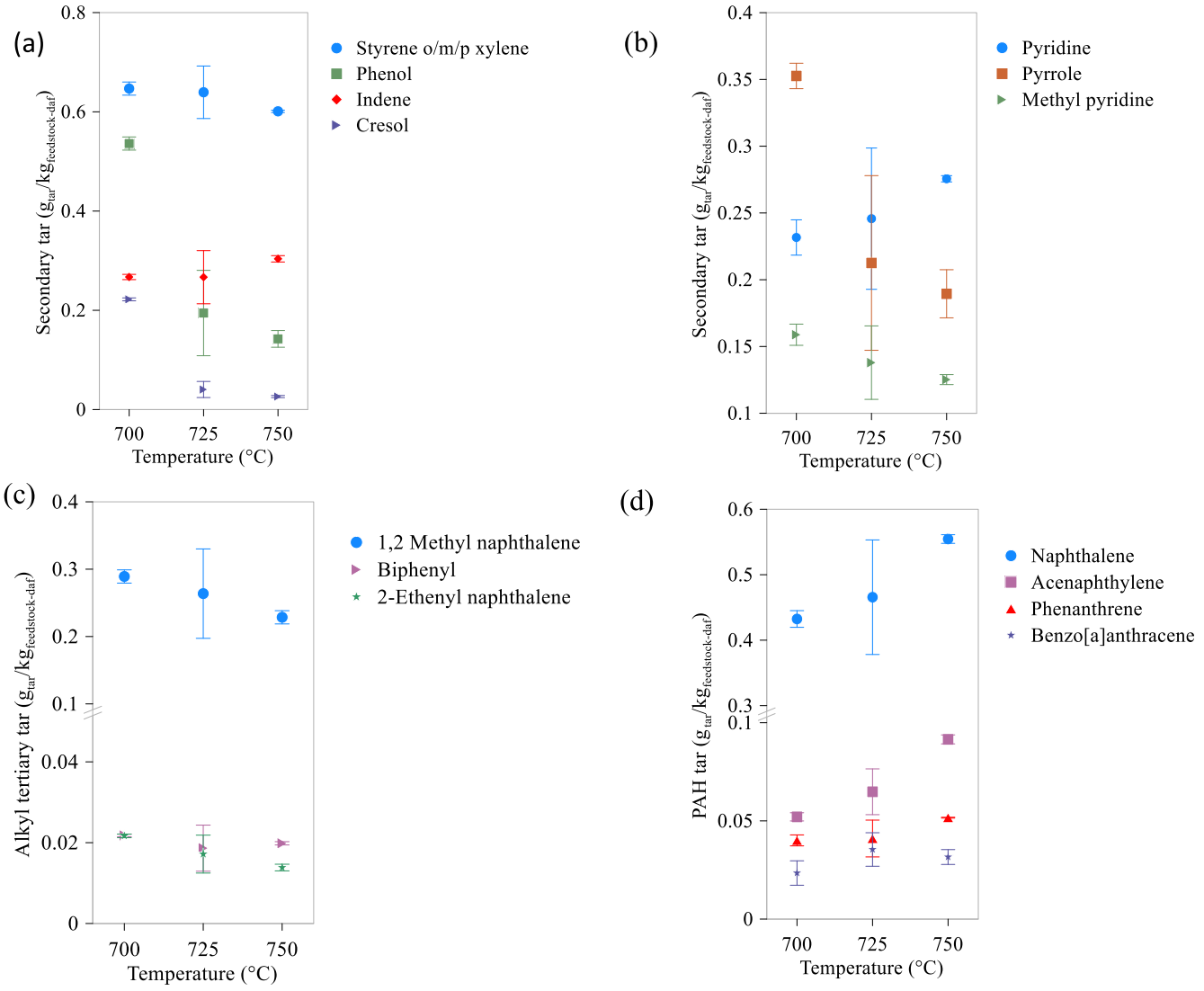

Fig. 5. Effect of temperature on the evolution of the most abundant individual tar compounds at an ER of 0.21.

thalene reduces slightly. Dufour et al. (2011) reported that reforming of methyl naphthalenes into naphthalene and acenaphthylene occurs at 800–900 °C. Horvat et al. (2016c) observed a peak in the yield at 800 °C for alkylated naphthalenes. Steady increase of biphenyl yield was observed at the temperature range 660–850 °C using torrefied feedstock. Biphenyl may act as an intermediate in the polymerisation pathway promoted by higher temperatures (Berrueco et al., 2014).

Tertiary PAH tar evolution shows an upward trend with rising temperature. The findings are in line with other researchers who observed that the production of PAH is driven by increased temperature (Horvat et al., 2016c; Berrueco et al., 2014). Yu et al. (2014) argued that at 850 °C the composition of tar consists mainly of PAHs. Naphthalene is the most abundant PAH compound ranging between 0.43 and 0.55 $g_{tar}/kg_{feedstock-daf}$. The low reforming rate of naphthalene is explained by its thermal stability. Naphthalene formation initiates either by the decomposition of heavier PAHs or by polymerisation reactions (Devi et al., 2005a; Nilsson et al., 2016). In this study the relatively low operating temperature resulted in low production of PAHs and the dominance of secondary tar.

3.4. Agglomeration issues

Agglomeration is a crucial phenomenon as regards the operational stability of fluidised bed gasifiers. The occurrence of bed agglomeration results in de-fluidisation conditions leading to local temperature and pressure deviations and consequent shutdown of the gasifier. The reason behind this phenomenon is the presence of inorganic compounds (P, K, Na, etc.) in the feedstock ash characterised by low melting temperatures. Agglomeration is exacerbated when silica sand is used as bed material as the reaction between silica and potassium may form low melting potassium silicate. Prevention or mitigation of such formation may be realised with the addition of calcium forming calcium phosphate instead with higher melting temperature (Pandey et al., 2016). Agglomeration in the first minutes of test 7 resulted in the interruption of the fluidisation conditions and feeding was stopped. After 10 min the feeding started again in order to investigate if the fluctuations appear again and although for 10 min (3–12 min in the Fig. S1 in supplementary file) the gasifier seemed to operate smoothly, deviations of pressure and temperature occurred again leading to the termination of the experiment.

4. Conclusions

The effect of temperature on the gasification behaviour of PL was experimentally studied in a lab-scale fluidised bed reactor. Gas yield, LCV and CGE showed an upward trend with increasing temperature from 700 °C to 750 °C. Although the LCV of 4.2 MJ/m^3 is low, if the presence of tar in the gas stream is taken into account represented as naphthalene, the value rises to 5.8 MJ/Nm^3, a fact that is useful if the product gas is destined directly for combustion without prior cleaning. Due to the high ash content of PL comprising of inorganic components characterised by low melting temperatures, agglomeration occurred at a temperature as low as 750 °C and ER 0.25. Total GC-detectable tar yield is expected to be lower compared to lignocellulosic biomass, due to both the low content of lignin in PL and the presence of inorganic compounds which act as tar reducting catalysts. Total GC-detectable tar yield decreased with temperature (from 5.6 $g_{tar}/kg_{feedstock\text{-}daf}$ at 700 °C to 4.25 $g_{tar}/kg_{feedstock\text{-}daf}$ at 750 °C). For the temperature range tested, secondary tar was the dominant category among the tar groups consisting of oxygen-containing phenolic compounds, substituted one-ring aromatics and nitrogen-containing hydrocarbons.

Despite the fact that the PL is considered a low-quality fuel, the present study reveals its potential as alternative energy resource for onsite (farm) energy generation. Nevertheless, increasing the operating temperature to improve the gasification performance while avoiding agglomeration conditions is a crucial aspect that needs to be further addressed. Addition of minerals in the fuel intake (use of additives) or mixing PL with conventional woody biomass that could change the ash composition are two viable options that can be further investigated as potential measures. On contrary to the lab-scale reactors that operate under allothermal conditions, industrial scale gasifiers operate in an autothermal mode implying that the reactor temperature is regulated by the ER. Therefore, modelling of the gasification process is proposed for future work in order to investigate if any of the conducted tests are close to auto-thermal conditions, which will provide the possibility to scale-up the experimental findings to an industrial gasifier level.

Acknowledgement

The authors would like to express their gratitude and appreciation to the European Commission for the financial support of the experimental campaign through the BRISK2 project (grant agreement number 731101) and to the staff of the Energy Research Centre of the Netherlands (ECN part of TNO) for hosting the experimental campaign. This work is supported by the Engineering and Physical Sciences Research Council (EPSRC, EP/P004636/1, UK). The financial support from EPSRC is gratefully acknowledged.

Appendix A. Supplementary material

Supplementary data to this article can be found online at https://doi.org/10.1016/j.wasman.2019.09.014.

References

Arena, U., 2012. Process and technological aspects of municipal solid waste gasification. A review. Waste Manage. 32, 625–639.
Arena, U., Di Gregorio, F., 2014. Energy generation by air gasification of two industrial plastic wastes in a pilot scale fluidized bed reactor. Energy 68, 735–743.
Arena, U., Di Gregorio, F., Santonastasi, M., 2010. A techno-economic comparison between two design configurations for a small scale, biomass-to-energy gasification based system. Chem. Eng. J. 162, 580–590.
Bartocci, P., Barbanera, M., D' Amico, M., Laranci, P., Cavalaglio, G., Gelosia, M., Ingles, D., Bidini, G., Buratti, C., Cotana, F., Fantozzi, F., 2017. Thermal degradation of driftwood: Determination of the concentration of sodium, calcium, magnesium, chlorine and sulfur containing compounds. Waste Manage. 60, 151–157.
Basu, P., 2010. Biomass Gasification and Pyrolysis: Practical Design and Theory. Academic Press.
Belgiorno, V., De Feo, G., Della Rocca, C., Napoli, R.M.A., 2003. Energy from gasification of solid wastes. Waste Manage. 23, 1–15.
Bernal, M.P., Bescós, B., Burgos, L., Bustamante, M., Clemente, R., Fabbri, C., Flotats Ripoll, X., García-González, M.C., Herrero Mallén, E., Mattachini, G., et al., 2015. Evaluation of manure management systems in Europe.
Berrueco, C., Montané, D., Güell, B.M., Del Alamo, G., 2014. Effect of temperature and dolomite on tar formation during gasification of torrefied biomass in a pressurized fluidized bed. Energy 66, 849–859.
Billen, P., Costa, J., Van der Aa, L., Van Caneghem, J., Vandecasteele, C., 2015. Electricity from poultry manure: a cleaner alternative to direct land application. J. Clean. Prod. 96, 467–475.
Burra, K., Hussein, M., Amano, R., Gupta, A., 2016. Syngas evolutionary behavior during chicken manure pyrolysis and air gasification. Appl. Energy 181, 408–415.
Cavalaglio, G., Coccia, V., Cotana, F., Gelosia, M., Nicolini, A., Petrozzi, A., 2018. Energy from poultry waste: an Aspen Plus-based approach to the thermo-chemical processes. Waste Manage. 73, 496–503.
Dalólio, F.S., da Silva, J.N., de Oliveira, A.C.C., Tinôco, I. de F.F., Barbosa, R.C., de Oliveira Resende, M., Albino, L.F.T., Coelho, S.T., 2017. Poultry litter as biomass energy: a review and future perspectives. Renew. Sustain. Energy Rev. 76, 941–949.
Devi, L., Ptasinski, K.J., Janssen, F.J., 2005a. Pretreated olivine as tar removal catalyst for biomass gasifiers: investigation using naphthalene as model biomass tar. Fuel Process. Technol. 86, 707–730.
Devi, L., Ptasinski, K.J., Janssen, F.J., van Paasen, S.V., Bergman, P.C., Kiel, J.H., 2005b. Catalytic decomposition of biomass tars: use of dolomite and untreated olivine. Renew. Energy 30, 565–587.
Di Gregorio, F., Santoro, D., Arena, U., 2014. The effect of ash composition on gasification of poultry wastes in a fluidized bed reactor. Waste Manage. Res. 32, 323–330.
Dufour, A., Masson, E., Girods, P., Rogaume, Y., Zoulalian, A., 2011. Evolution of aromatic tar composition in relation to methane and ethylene from biomass pyrolysis-gasification. Energy Fuels 25, 4182–4189.
Font Palma, C., Martin, A.D., 2013. Model based evaluation of six energy integration schemes applied to a small-scale gasification process for power generation. Biomass Bioenergy 54, 201–210.
Horvat, A., Kwapinska, M., Xue, G., Dooley, S., Kwapinski, W., Leahy, J.J., 2016a. Detailed measurement uncertainty analysis of solid-phase adsorption-total gas chromatography (GC)-detectable tar from biomass gasification. Energy Fuels 30, 2187–2197.
Horvat, A., Kwapinska, M., Xue, G., Kwapinski, W., Dooley, S., Leahy, J., 2016b. Study of post sampling treatment of solid phase adsorption method on tar yields and comparison of two methods for volatile tar compounds. In: Proceedings 24th European biomass conference and exhibition, pp. 929–933.
Horvat, A., Kwapinska, M., Xue, G., Rabou, L.P., Pandey, D.S., Kwapinski, W., Leahy, J. J., 2016c. Tars from fluidized bed gasification of raw and torrefied Miscanthus x giganteus. Energy Fuels 30, 5693–5704.
Huang, Y., Anderson, M., McIlveen-Wright, D., Lyons, G., McRoberts, W., Wang, Y., Roskilly, A., Hewitt, N., 2015. Biochar and renewable energy generation from poultry litter waste: a technical and economic analysis based on computational simulations. Appl. Energy 160, 656–663.
Israelsson, M., Seemann, M., Thunman, H., 2013. Assessment of the solid-phase adsorption method for sampling biomass-derived tar in industrial environments. Energy Fuels 27, 7569–7578.
Joseph, P., Tretsiakova-McNally, S., McKenna, S., 2012. Characterization of cellulosic wastes and gasification products from chicken farms. Waste Manage. 32, 701–709.
Kiel, J., Van Paasen, S., Neeft, J., Devi, L., Ptasinski, K., Janssen, F., Meijer, R., Berends, R., Temmink, H., Brem, G., et al., 2004. Primary measures to reduce tar formation in fluidised-bed biomass gasifiers. ECN, ECN-C-04-014.
Kim, Y.D., Yang, C.W., Kim, B.J., Kim, K.S., Lee, J.W., Moon, J.H., Yang, W., Tae, U.Y., Do Lee, U., 2013. Air-blown gasification of woody biomass in a bubbling fluidized bed gasifier. Appl. Energy 112, 414–420.
Lynch, D., Henihan, A.M., Bowen, B., Lynch, D., McDonnell, K., Kwapinski, W., Leahy, J.J., 2013. Utilisation of poultry litter as an energy feedstock. Biomass Bioenergy 49, 197–204.
Milne, T.A., Evans, R.J., Abatzoglou, N., 1997. Biomass gasifier "tars": their nature, formation, destruction, and tolerance limits in energy conversion devices. Making Bus. Biomass Energy, Environ., Chem., Fibers Mater. 1, 729–738.
Molino, A., Chianese, S., Musmarra, D., 2016. Biomass gasification technology: the state of the art overview. J. Energy Chem. 25, 10–25.
Neubert, M., Reil, S., Wolff, M., Pocher, D., Stork, H., Ultsch, C., Meiler, M., Messer, J., Kinzler, L., Dillig, M., Beer, S., Karl, J., 2017. Experimental comparison of solid phase adsorption (SPA), activated carbon test tubes and tar protocol (DIN CEN/TS 15439) for tar analysis of biomass derived syngas. Biomass Bioenergy 105, 443–452.
Nilsson, S., Gómez-Barea, A., Fuentes-Cano, D., Haro, P., Pinna-Hernández, G., 2016. Gasification of olive tree pruning in fluidized bed: experiments in a laboratory-scale plant and scale-up to industrial operation. Energy Fuels 31, 542–554.

Padban, N., Wang, W., Ye, Z., Bjerle, I., Odenbrand, I., 2000. Tar formation in pressurized fluidized bed air gasification of woody biomass. Energy Fuels 14, 603–611.

Pan, I., Pandey, D.S., 2016. Incorporating uncertainty in data driven regression models of fluidized bed gasification: a Bayesian approach. Fuel Process. Technol. 142, 305–314.

Pandey, D.S., Kwapinska, M., Gómez-Barea, A., Horvat, A., Fryda, L.E., Rabou, L.P., Leahy, J.J., Kwapinski, W., 2016. Poultry litter gasification in a fluidized bed reactor: effects of gasifying agent and limestone addition. Energy Fuels 30, 3085–3096.

Rabou, L.P., Zwart, R.W., Vreugdenhil, B.J., Bos, L., 2009. Tar in biomass producer gas, the Energy research Centre of the Netherlands (ECN) experience: an enduring challenge. Energy Fuels 23, 6189–6198.

Rios, M.L.V., González, A.M., Lora, E.E.S., del Olmo, O.A.A., 2018. Reduction of tar generated during biomass gasification: a review. Biomass Bioenergy 108, 345–370.

Rumsey, J., 2018. United Kingdom Poultry and Poultry Meat Statistics - August 2018.

Tar dew point [WWW Document], n.d. URL http://www.thersites.nl/tardewpoint.aspx (accessed 11.21.18).

Taupe, N., Lynch, D., Wnetrzak, R., Kwapinska, M., Kwapinski, W., Leahy, J.J., 2016. Updraft gasification of poultry litter at farm-scale-a case study. Waste Manage. 50, 324–333.

Van Paasen, S., Kiel, J., 2004. Tar formation in a fluidised-bed gasifier: Impact of fuel properties and operating conditions. Energy Research Centre of the Netherlands ECN.

Wen, C., Yu, Y., 1966. A generalized method for predicting the minimum fluidization velocity. AIChE J. 12, 610–612.

Xue, G., Kwapinska, M., Horvat, A., Kwapinski, W., Rabou, L., Dooley, S., Czajka, K., Leahy, J.J., 2014. Gasification of torrefied Miscanthus x giganteus in an air-blown bubbling fluidized bed gasifier. Bioresour. Technol. 159, 397–403.

Yu, H., Zhang, Z., Li, Z., Chen, D., 2014. Characteristics of tar formation during cellulose, hemicellulose and lignin gasification. Fuel 118, 250–256.

Zhao, Q., Wang, X., Tan, H., Si, J., Niu, Y., Xu, T., 2010. Co-pyrolysis of pyridine and pyrrole as nitrogenous compounds model of coal. Asian J. Chem. 22, 6998.